Nuclear Physics B45 (1972) 217–236. North-Holland Publishing Company

INCLUSIVE HADRON SPECTRA AND THE MULTIPERIPHERAL MODEL

P. RIPA
CNEA-Ciclotrón, Av. del Libertador 8250, Buenos Aires, Argentina

Received 6 April 1972

Abstract: A simplified version of the MP model developed by DeTar is improved so as to reproduce the experimental fragmentation spectrum. The model is then used to study the effect of introducing Pomeron exchange in the MP chain. Scaling behavior is shown to hold even at $x = 0$, where an inverted cusp of the form $A + B\sqrt{|x|}$ in the scaling function is found. This structure is in general related to non-leading trajectories and is shown to be present in Mueller's analysis and in other MP models without pomeron exchange. In the latter the amount of cusp is related to the coupling between different (input) channels. Non-scaling contributions, two-particle inclusive spectra and triple Regge limit are also discussed.

1. INTRODUCTION

At high energy the inelastic events account for a large fraction of the hadron–hadron total cross section.

The theoretical and experimental difficulty in the study of a particular (exclusive) process with production of many particles has drawn attention to the inclusive processes of the type [1]

$$a + b \to c_1 + c_2 + \ldots + c_n + X, \tag{1}$$

where $c_1 \ldots c_n$ is a specified set of n observed particles, and X denotes the summation over all allowed hadron states.

The case $n = 0$ corresponds to the total cross section and the case $n = 1$ to single particle distributions described by the function *

$$\rho^{c}_{ab}(p_\perp, p_\parallel, s) = \frac{E^c}{\sigma^{tot}_{ab}(s)} \frac{d\sigma_{ab}}{d^3P_c}, \tag{2}$$

where $s^{\frac{1}{2}}$ is the total c.m. energy.

* Throughout this paper we work in frames in which the momenta of particles a and b are collinear. Longitudinal components are measured in the direction of $\boldsymbol{p}_b - \boldsymbol{p}_a$.

The scaling conjecture [1] states that as $s \to \infty$, ρ_{ab}^{c} becomes a function of only $p_\perp$ and the c.m. longitudinal fraction $x = 2p_\parallel s^{-\frac{1}{2}}$, namely

$$\lim_{s\to\infty} \rho_{ab}^{c}(p_\perp, p_\parallel, s) = f_{ab}^{c}(p_\perp, x). \tag{3}$$

In addition

$$\begin{aligned} &f_{ab}^{c}(p_\perp, x) = f_{b}^{c}(p_\perp, x) && x > 0 \\ &f_{ab}^{c}(p_\perp, 0) = f^{c}(p_\perp) && \\ &f_{ab}^{c}(p_\perp, x) = f_{a}^{c}(p_\perp, -x) && x < 0. \end{aligned} \tag{4}$$

Division by σ_{ab}^{tot} in eq. (2) makes it possible for ρ_{ab}^{c} to scale even if σ_{ab}^{tot} vanishes or diverges as $s \to \infty$. This can be seen from the relation

$$\sum_{c} \int\int \rho_{ab}^{c}(p_\perp, x, s)\, dx\, d^2p_\perp = 2$$

derived from energy conservation.

Furthermore, the simple form of relations (4) does not hold if the division by σ_{ab}^{tot} in eq. (2) is not performed.

An important consequence of scaling and the limitation of transverse momenta is the logarithmic growth of the average multiplicity of particle c at large values of s

$$\bar{n}_c = a_c \ln(s/s_0) + b_{ab}^{c}, \tag{5}$$

where

$$a_c = \int d^2\boldsymbol{p}_\perp f^{c}(p_\perp)$$

$$b_{ab}^{c} = \int d^2\boldsymbol{p}_\perp \left[\int \frac{dx}{|x|} \left(f_{ab}^{c}(p_\perp, x) - f^{c}(p_\perp)\right) - f^{c}(p_\perp) \ln(s_0/4\omega_c^2) \right], \tag{6}$$

and $\omega_c = (m_c^2 + p_\perp^2)^{\frac{1}{2}}$ is the longitudinal mass of particle c.

To obtain eq. (5) it is sufficient to assume uniform converge for the limit of eq. (3) and the existence of the integrals in eq. (6). Both conditions are satisfied in the model described below, even though f_{ab}^{c} turns out not to be analytic at $x = 0$.

A very useful variable is the rapidity

$$y = \mathrm{th}^{-1}(p_\parallel/E). \tag{7}$$

Since $d^3\boldsymbol{p}/E = d^2\boldsymbol{p}_\perp dy$, a longitudinal boost is only a shift of the origin of rapidities and thus differences of rapidities are invariant under those transformations.

We can write

$$s = m_a^2 + m_b^2 + 2m_a m_b \cosh y \cong m_a m_b\, e^{Y} \tag{8}$$

where $Y = y_b - y_a$.

Conjectures (3) and (4) can be shown to be equivalent to saying that ρ_{ab}^{c} becomes, as $Y \to \infty$:

(i) independent of y_b and the nature of particle b if $y_c - y_a$ remains finite. This is called fragmentation of a into c [2]. A reciprocal statement can be made about b when $y_b - y_c$ remains finite.

(ii) a function of only c and p when $y^c_{c.m.}$ remains finite. This region is called pionization.

The properties discussed above can be deduced from detailed (microscopic) models of production amplitudes or from (macroscopic) models for forward exclusive processes which can be related to inclusive cross sections via generalized optical theorems [3].

De Tar [4] developed a MP model working in rapidity variable and ignoring transverse momenta, which has a platean in the pionization region and falls abruptly at both fragmentation ends. This model is modified in sect. 2 so as to improve the behavior in the fragmentation regions, and then used in sect. 3 to fit the $p + p \to \pi^- + X$ spectrum at 30 GeV, allowing pomeron and meson exchanges.

The fit predicts the appearance of a dip around $x = 0$ at higher energies, which becomes an inverted cusp in the scaling function as $s \to \infty$. This structure is shown, in sect. 3, to be present in Mueller's analysis and in MP models with no pomeron exchange.

Scaling predictions of the MP model are discussed in the same section for certain processes that are neither exclusive nor inclusive and in sect. 4 for two-particle inclusive processes.

Finally, in sect. 5, the model is improved with the introduction of transverse momenta and predictions for the triple Regge are discussed.

2. MULTIPERIPHERAL MODEL

The basic assumptions of the MP model [5] for the production amplitude (fig.1) are

(a) Limitation of the invariant momentum transfers t_i.

(b) Lack of correlations between distant particles in the MP chain.

As we will see below assumption (a) leads to a limitation of the transverse momenta. Therefore, following De Tar [4], we ignore transverse momenta* and write

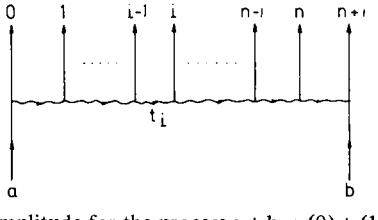

Fig. 1. MP amplitude for the process $a + b \to (0) + (1) + \ldots (n + 1)$.

* Longitudinal spectra can then be thought to correspond either to an average $\langle p^c_\perp \rangle$ or to distributions integrated over $d^2 p^c_\perp$.

for the n-particle production cross section

$$\sigma_{ab}^{n}(Y) = \lambda^{-\frac{1}{2}}(s, m_a^2, m_b^2) \int |M|^2 \, dR_{n+2}^{L} \tag{9}$$

The longitudinal phase space is given by

$$\begin{aligned} dR_{n+2}^{L} &= \delta(m_a e^{y_a} + m_b e^{y_b} - \sum_{0}^{n+1} \bar{\omega}_i e^{y_i}) \\ &\quad \delta(m_a e^{-y_a} + m_b e^{-y_b} - \sum_{0}^{n+1} \omega_i e^{-y_i}) \prod_{0}^{n+1} dy_i \\ &= \lambda^{-\frac{1}{2}}(W^2, \bar{\omega}_0^2, \bar{\omega}_{n+1}^2) \, \delta(y_0 - y_a - \epsilon_a) \, \delta(y_b - y_{n+1} - \epsilon_b) \prod_{0}^{n+1} dy_i, \end{aligned} \tag{10}$$

where

$$W^2 = (m_a e^{y_a} + m_b e^{y_b} - \sum_{1}^{n} \bar{\omega}_i e^{y_i}) (m_a e^{-y_a} + m_b e^{-y_b} - \sum_{1}^{n} \bar{\omega}_i e^{-y_i})$$

is the square of the longitudinal mass of the (0) + (n+1) particles system and

$$\epsilon_a = \mathrm{ch}^{-1} \left(\frac{s + m_a^2 - m_b^2}{2\sqrt{s}\, m_a} \right) - \mathrm{ch}^{-1} \left(\frac{W^2 + \bar{\omega}_0^2 - \bar{\omega}_{n+1}^2}{2 W \bar{\omega}_0} \right) \tag{11}$$

with the same expression for ϵ_b making $0 \leftrightarrow n+1$, $a \leftrightarrow b$.

Longitudinal Lorentz invariance requires the amplitude M, depicted by the diagram of fig. 1, to depend on differences of rapidities. Assuming minimal correlations we can write

$$\begin{aligned} &|M|^2 \lambda^{-\frac{1}{2}}(s, m_a^2, m_b^2) \lambda^{-\frac{1}{2}}(W^2, \bar{\omega}_0^2, \bar{\omega}_{n+1}^2) = \\ &G_a^2(y_0 - y_a) \, K_{01}(y_1 - y_0) g_1^2 \cdots K_{n\,n+1}(y_{n+1} - y_n) \, \tilde{G}_b^2. \end{aligned} \tag{12}$$

If we allow for N different kinds of exchanges, the external vertices G_a^2 and $\tilde{G}_b^2$ are N component row and column vectors respectively, the propagators K_{ij} are $N \times N$ diagonal matrices and the internal vertex $g^2 = \Sigma_i g_i^2$ is a $N \times N$ symmetric matrix.

In order to find an expression for the kernel we make the following considerations:

(i) At large values of $Z_i = y_i - y_{i-1}$ the subenergies $s_{i\,i-1}$ are given by

$$s_{i\,i-1} \cong \omega_i \, \omega_{i-1} \, e^{Z_i}. \tag{13}$$

Therefore, multi Regge behavior requires, at large Z

$$K_{i\,i-1}(Z) \cong e^{-\beta Z} \tag{14}$$

with $\beta = 2 - 2\bar{\alpha}$, where $\bar{\alpha}$ is the (average) value of the exchanged Regge trajectory.

(ii) For the behavior at small values of Z_i we go back to the assumption of limitation of the invariant momentum transfers. In terms of the variables y and $p_\perp$, these can be written as [4]

$$t_i = -\left(\sum_{j=0}^{i-1} \omega_j e^{y_j - m_a} e^{y_a}\right)\left(\sum_{j=i}^{n+1} \omega_j e^{-y_j - m_b} e^{-y_b}\right) - \left(\sum_{j=0}^{i-1} p_j^{\perp}\right)^2. \quad (15)$$

We observe that assumption (a) leads to

(i) The limitation of $p_\perp$ used above.

(ii) An ordered distribution of y_i [6].

The leading term in (15) contains the following dependence on the relative relativity Z_i

$$t_i = -\bar{\omega}_i \bar{\omega}_{i-1} e^{-Z_i} - \left(\sum_{j=0}^{i-1} p_j^{\perp}\right)^2. \quad (16)$$

Therefore an exponential damping in t_i would approximately lead to a kernel

$$K_{ij}(Z) = e^{-b\bar{\omega}_i \bar{\omega}_j e^{-Z}} e^{-\beta Z}. \quad (17)$$

This kernel cuts off rapidly for negative values of Z. Because it is difficult to iterate analytically we use instead

$$K_{ij}(Z) = \bar{\theta}(Z - \bar{\eta}_i - \bar{\eta}_j) e^{-\beta Z} \quad (18)$$

where $\bar{\theta}(v)$ is some cut off function and $\bar{\eta}_i - \bar{\eta}_j \cong \ln(\bar{\omega}_i/\bar{\omega}_j)$.

In ref. [4] only production of pions was considered, $\bar{\theta}(v)$ was chosen to be a step function at the origin and $Z\bar{\eta}_\pi$ was set to zero. These approximations lead to a rectangular inclusive pion spectrum, which is too rough an approximation in the fragmentation regions. Therefore, in order to construct a more realistic kernel, in an earlier paper [7] we shifted the step from the origin and let it have a linear increase with a certain width. Here we use a even smoother parametrization which reproduces better the behavior of eq. (17)

$$\bar{\theta}(v) = \theta(v)\,(1 - (1 + v/a)\exp(-v/a)). \quad (19)$$

In this section we also assume that only pions are produced and concentrate on the spectrum of the pions emitted at internal vertices in the MP chain.

Therefore we integrate over dy_0 and dy_{n+1} using the δ functions in (10) which give

$$y_0 = y_a + \epsilon_a, \quad y_{n+1} = y_b - \epsilon_b. \quad (20)$$

From (11) and conclusion (ii) we observe that in the MP region, and for diagrams with $\bar{\omega}_0 \geqslant m_a$ and $\bar{\omega}_{n+1} \geqslant m_b$, ϵ_a and ϵ_b are approximately independent of y_i, so we set them to average values

$$\epsilon_a = \bar{\epsilon}_a \gtrsim \ln \frac{\bar{\omega}_0}{m_a}, \quad \epsilon_b = \bar{\epsilon}_b \gtrsim \ln \frac{\bar{\omega}_{n+1}}{m_b}. \quad (21)$$

We thus obtain from eq. (9), (10), (12), (18) and (21).

$$\sigma_{ab}^{n}(Y) = G_a^2 A^n(Y - \bar{\Delta}_a - \bar{\Delta}_b)\,\tilde{G}_b^2,$$
$$\sigma_{ab}^{tot}(Y) = G_a^2 A(Y - \bar{\Delta}_a - \bar{\Delta}_b)\,\tilde{G}_b^2, \tag{22}$$

where $\bar{\Delta}_i = \bar{\epsilon}_i + \bar{\eta}_i - \bar{\eta}_\pi$ and the matrices $A^n(Z)$ and $A(Z) = \Sigma_0^\infty A^n(Z)$ are obtained from

$$A^n(z) = \int K(Z_1) g^2 K(Z_2) \ldots K(Z_{n+1})\, \delta(Z - Z_1 - \ldots Z_{n+1})\, dZ_1 \ldots dZ_{n+1}, \tag{23}$$

$$A(Z) = K(Z) + \int A(Z') g^2 K(Z - Z')\, dZ' \tag{24}$$

with $K(Z) = K_{\pi\pi}(Z)$.

This integral equation, contracted with G_a^2, is shown in fig. 2a.

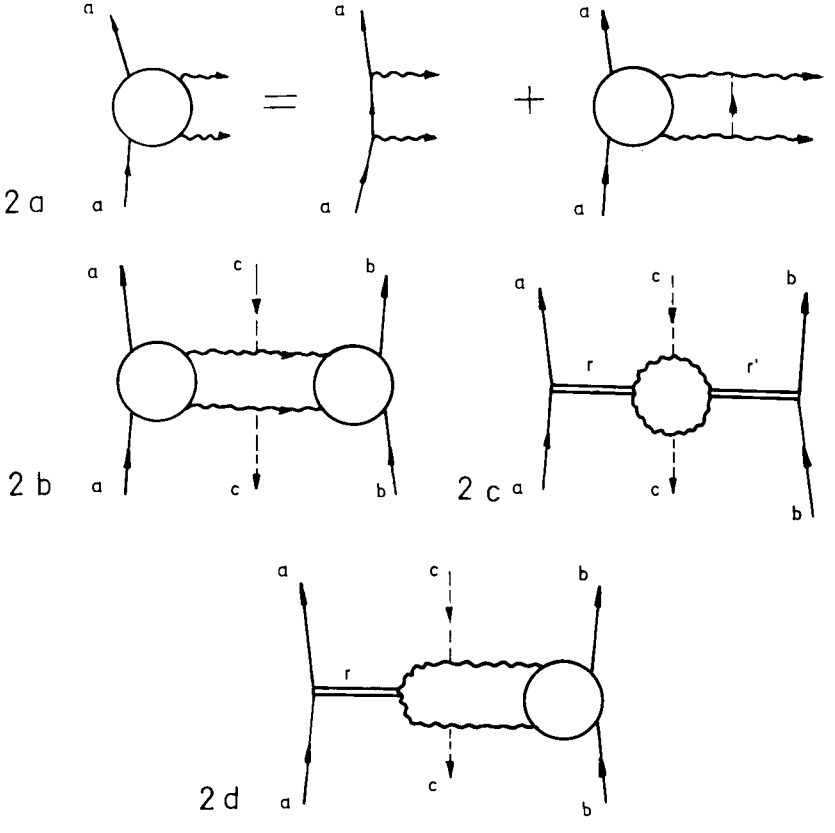

Fig. 2. (a) The integral equation $G_a^2 A = G_a^2 K + G_a^2 A g^2 K$. (b) Cross section for a + b → c + X. (c) Central part of spectrum. (d) Scaling function f_b^c ($r = \mathbb{P}$) or non-scaling contribution g_{ab}^c ($r = R$) for positive values of x. Solid and broken lines are external particles, wiggly lines are input reggeons and double lines are output reggeons.

The spectrum of the i^{th} pion when n pions are produced is

$$\frac{\mathrm{d}\sigma_{\mathrm{ab}}^{n}}{\mathrm{d}y_i} = G_{\mathrm{a}}^2\, A^{i-1}(y_i - y_{\mathrm{a}} - \bar{\Delta}_{\mathrm{a}}) g^2 A^{n-i}\,(y_{\mathrm{b}} - y_i - \bar{\Delta}_{\mathrm{b}})\, \tilde{G}_{\mathrm{b}}^2. \tag{25}$$

Summing over i and n we get the inclusive pion spectrum (see fig. 2 b)

$$\frac{\mathrm{d}\sigma_{\mathrm{ab}}}{\mathrm{d}y_\pi} = G_{\mathrm{a}}^2 A(y_\pi - y_{\mathrm{a}} - \bar{\Delta}_{\mathrm{a}}) g^2 A(y_{\mathrm{b}} - y_\pi - \bar{\Delta}_{\mathrm{b}})\, \tilde{G}_{\mathrm{b}}^2. \tag{26}$$

Eq. (24) can be solved by iterations or by performing a Fourier transform. The first method is good for small Z whereas the second one is better to study the large Z behavior, namely

$$a(\varphi) = k(\varphi) + a(\varphi) g^2 k(\varphi) = 1/(k^{-1}(\varphi) - g^2) \tag{27}$$

with $a(\varphi) = \int A(Z) \exp(-i\varphi Z)\, \mathrm{d}Z$, and similarly for $k(\varphi)$.

Then, if $\det(k^{-1}(\varphi) - g^2) = 0$ for $\varphi = i\mu_r$, we have for $\varphi \cong i\mu_r$

$$a(\varphi) = \frac{C_r \otimes C_r^{\mathrm{T}}}{2\pi i(\varphi - i\mu_r)}, \tag{28}$$

with C_r a (constant) N-component row vector.

Then, at large Z

$$A(Z) \sim \sum_r \mathrm{e}^{-\mu_r Z}\, C_r \otimes C_r^{\mathrm{T}}, \tag{29}$$

and, with eq.(22) *

$$\sigma_{\mathrm{ab}}^{\mathrm{tot}}(Y) \sim \sum_r \gamma_{\mathrm{a}}^r \tilde{\gamma}_{\mathrm{b}}^r\, \mathrm{e}^{-\mu_r Y} \cong \sum_r \gamma_{\mathrm{a}}^r \gamma_{\mathrm{b}}^r\, (s/m_{\mathrm{a}} m_{\mathrm{b}})^{-\mu_r} \tag{30}$$

where

$$\gamma_{\mathrm{a}}^r = G_{\mathrm{a}}^2 \cdot C_r\, \mathrm{e}^{\mu_r \bar{\Delta}} \mathrm{a}, \qquad \tilde{\gamma}_{\mathrm{b}}^r = C_r^{\mathrm{T}} \cdot \tilde{G}_{\mathrm{b}}^2\, \mathrm{e}^{\mu_r \bar{\Delta}} \mathrm{b} \tag{31}$$

The factorized form of the residues in eq. (29) and (30) follows from the symmetry of the matrix $k^{-1} - g^2$ [8].

As for the inclusive cross section for $y_\pi \gg y_{\mathrm{a}}$ and $y_\pi \ll y_{\mathrm{b}}$ we have

$$\frac{\mathrm{d}\sigma_{\mathrm{ab}}}{\mathrm{d}y_\pi} \cong \sum_{rr'} \gamma_{\mathrm{a}}^r \tilde{\gamma}_{\mathrm{b}}^{r'}\, C_r g^2 C_{r'}^{\mathrm{T}}\, \mathrm{e}^{-\mu_r(y_\pi - y_{\mathrm{a}}) - \mu_{r'}(y_{\mathrm{b}} - y_\pi)} \tag{32}$$

$$\cong \sum_{rr'} \gamma_{\mathrm{a}}^r \tilde{\gamma}_{\mathrm{b}}^{r'}\, C_r g^2 C_{r'}^{\mathrm{T}}\, (m_{\mathrm{a}}(\bar{x}+x)/2\bar{\omega}_\pi)^{\mu_r} (m_{\mathrm{b}}(\bar{x}-x)/2\bar{\omega}_\pi)^{\mu_{r'}},$$

where $\bar{x} = (x^2 + 4\bar{\omega}_\pi^2/s)^{\frac{1}{2}}$, as depicted in fig. 2c.

* So a Regge pole $\alpha_r(t)$ in the elastic ab amplitude corresponds to $\alpha_r(0) = 1 - \mu_r$.

Experimentally one pole with intercept close to one and several poles with intercept close to 0.5 are found in the elastic amplitude. In a model with N exchanges we can choose the internal parameters so as to get in eq. (29) one pole with $\mu \sim 0, N-1$ poles with $\mu \sim 0.5$ and the other poles, if any, with $\mathrm{Re}\mu \geqslant 1$. We denote the first by $\mathbb{P}$ (output pomeron) and the second set by R. Then eq. (30) becomes

$$\sigma_{ab}^{tot}(Y) = e^{-\mu_{\mathbb{P}} Y}(\gamma_a^{\mathbb{P}} \tilde{\gamma}_b^{\mathbb{P}} + e^{-\frac{1}{2}Y} \sum_R \gamma_a^R \tilde{\gamma}_b^R) + O(e^{-Y}). \tag{33}$$

We observe also that the inclusive spectrum (26) has scaling behavior as defined in eq. (3) and (4) with *

$$f_i^{\pi}(x) = \frac{1}{\gamma_i^{\mathbb{P}}} (\bar{\omega}_{\pi}/m_i x)^{\mu_{\mathbb{P}}} G_i^2 A(\ln \frac{\bar{\omega}_{\pi}}{m_i x} - \bar{\Delta}_i) g^2 C_{\mathbb{P}}^T \tag{34}$$

$$f_i^{\pi}(O) = f^{\pi} = C_{\mathbb{P}} g^2 \; C_{\mathbb{P}}^T,$$

as depicted in fig. 2d, with $r = \mathbb{P}$.

At small values of x the scaling function has the structure

$$\begin{aligned} f_i^{\pi}(x) &\sim \sum_r \frac{\gamma_i^r}{\gamma_i^{\mathbb{P}}} C_r g^2 \; C_{\mathbb{P}}^T \, (m_i x/\bar{\omega}_{\pi})^{\mu_r - \mu_{\mathbb{P}}} \\ &= f^{\pi} + \delta_i^{\pi} \sqrt{\frac{m_i x}{\bar{\omega}_{\pi}}} + O(x) \end{aligned} \tag{35}$$

where

$$\delta_i^{\pi} = \sum_R \frac{\gamma_i^R}{\gamma_i^{\mathbb{P}}} C_R g^2 C_{\mathbb{P}}^T. \tag{36}$$

as depicted in fig. 2c with $r = \mathbb{P}$, $r' = R$ ($r = R$, $r' = \mathbb{P}$) for positive (negative) values of x.

So we expect $f_{ab}^c(x)$ not to be analytic at $x = 0$, and to have a $\sqrt{|x|}$ like cusp at this point unless δ_a^c and δ_b^c vanish. This is not surprising since properties (4) cannot be achieved if f_{ab}^c is analytic at $x = 0$, except if f_{ab}^c is also independent of both particles a and b away from $x = 0$.

The above statement is about the scaling function f_{ab}^c; in this model both ρ_{ab}^c and $(d/dx)\rho_{ab}^c$ are continuous functions of x at any finite value of s.

With respect to the rate at which the scaling limit is approached we observe that

$$\begin{aligned} &\rho_{ab}^c(p_{\perp}, x, s) - f_{ab}^c(p_{\perp}, x) = O(s^{-\frac{1}{2}}) \quad x \neq 0, \\ &\rho_{ab}^c(p_{\perp}, 0, s) - f^c(p_{\perp}) = O(s^{-\frac{1}{4}}). \end{aligned} \tag{37}$$

* Indeed the x-spectrum cannot be obtained from the y-spectrum after integration over $d^2 p_{\perp}^c$. However, we suppose that the shape of the first is approximately the same as that obtained from $\rho(y, p_{\perp})$ at an average value of $\langle p_{\perp} \rangle$. This is justified in sect. 6.

More precisely, in our case

$$\rho^{\pi}_{ab}(0, s) - f^{\pi} = (\delta^{\pi}_{a}\sqrt{m_a} + \delta^{\pi}_{b}\sqrt{m_b})\, s^{-\frac{1}{4}}, \tag{38}$$

$$\rho^{\pi}_{ab}(x, s) - f^{\pi}_{ab}(x) = e^{-\frac{1}{2}Y}\left(g^{\pi}_{ab}(x) - \sum_{R} \frac{\gamma^{R}_{a}\tilde{\gamma}^{R}_{b}}{\gamma^{\mathbb{P}}_{a}\gamma^{\mathbb{P}}_{b}}\right) + O(e^{-Y}),$$

where

$$g^{\pi}_{ab}(x) = \sum_{R} (\psi_i)^{\mu_R} \frac{\gamma^{R}_{j}}{\gamma^{\mathbb{P}}_{a}\gamma^{\mathbb{P}}_{b}} G^2_a A(\ln(\psi_i) - \bar{\Delta}_i) g^2\, C^{T}_{R}, \tag{39}$$

with $\psi_i = \bar{\omega}_{\pi}/m_i\,|x|$, as depicted in fig. 2d with $i = b, j = a$ ($i = a, j = b$) for positive (negative) values of x.

At small values of x we obtain

$$g^{\pi}_{ab}(x) \sim \delta^{\pi}_{j}(\bar{\omega}_{\pi}/m_i|x|)^{\frac{1}{2}} \tag{40}$$

as depicted in fig. 2c with $r = R, r' = \mathbb{P}$ ($r = \mathbb{P}, r' = R$) for positive (negative) values of x.

Eqs. (38) and (40) show that the scaling limit is approached more slowly at smaller values of $|x|$.

We want to point out that in this model g^{π}_{ab} can be negative, for certain values of x, since in eq. (39) both γ^{R}_{i} and some components of C_R can be negative. This means that at certain values of x the scaling limit can be approached from below even though the total cross-section approaches its asymptotic value from above. This last property can be achieved in the model through a positive value of $\Sigma_R\, \gamma^{R}_{a}\tilde{\gamma}^{R}_{b}$.

3. MODEL WITH TWO EXCHANGES

Let us use the results of the last section to discuss a model with an average meson (M) and pomeron * (P) exchanges [9].

The model is then given by

$$K(Z) = \begin{pmatrix} K_P(Z) & 0 \\ 0 & K_M(Z) \end{pmatrix} \qquad g^2 = \begin{pmatrix} 0 & g^2_{PM} \\ g^2_{PM} & g^2_{MM} \end{pmatrix}, \tag{41}$$

$$G^2_a \equiv (\tilde{G}^2_a)^T = (G^2_{a,P} \quad G^2_{a,M}).$$

We fit the $p + p \to \pi^- + X$ spectrum at 30 GeV constraining the internal parameters to obtain $\mu_1 = \mu_{\mathbb{P}} = 0$ and $\mu_2 = \mu_R = 0.5$; and the external vertices to yield $\sigma^{tot}_{pp}(Y) \cong \sigma^{tot}_{pp}(\infty)(1 + 0.4\exp(-\frac{1}{2}Y))$.

* We distinguish here between the input pomeron (P) and the output pomeron ($\mathbb{P}$) discussed in sect. 2. We ignore the problem of self-consistency between output and input poles since the former are evaluated at $t = 0$ and the latter should be taken at an average value $t < 0$.

The fit gives $\beta_P = 0.135$ and $\beta_M = 1.57$, corresponding to average exchanges of $\bar{\alpha}_P = 0.932$ and $\bar{\alpha}_M = 0.27$.

For the range and the different cut-offs of the kernels we obtain $a = 1.43$, $\bar{\Delta}_N = 1.0$ and $\bar{\eta}_\pi = -0.43$. This negative value of $\bar{\eta}_\pi$ implies a non-vanishing contribution from regions of phase space where consecutive points are "crossed", i.e., $y_i < y_{i-1}$.

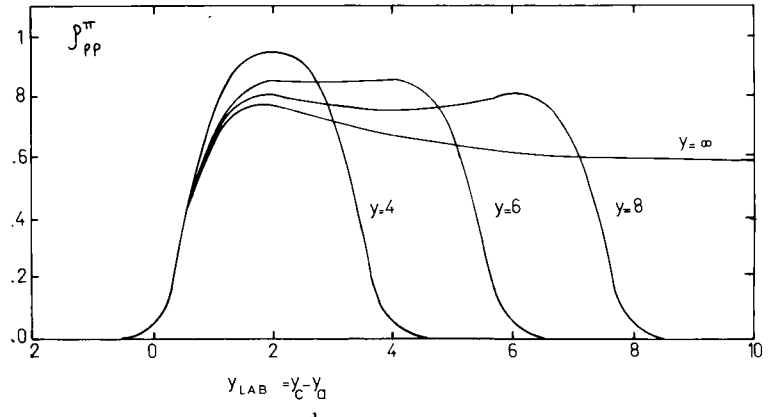

Fig. 3. Inclusive spectrum $\rho^{\pi}_{pp} = \frac{1}{\sigma_{pp}} \frac{d\sigma_{pp\to\pi X}}{dy_\pi}$ as a function of y_π in the lab frame.

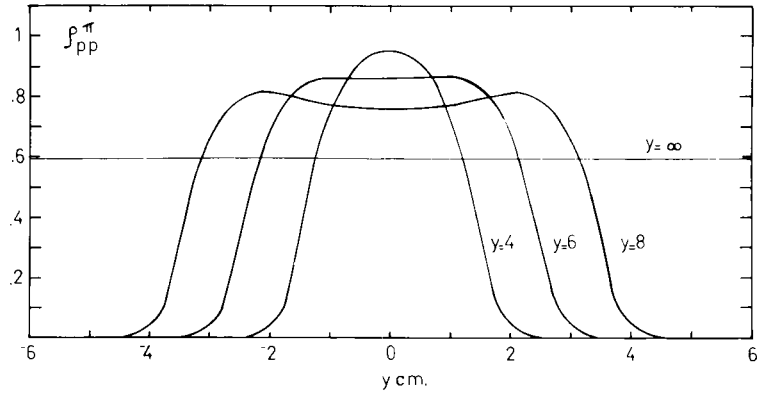

Fig. 4. Inclusive spectrum of fig. 3 as a function of y_π in the c.m. frame.

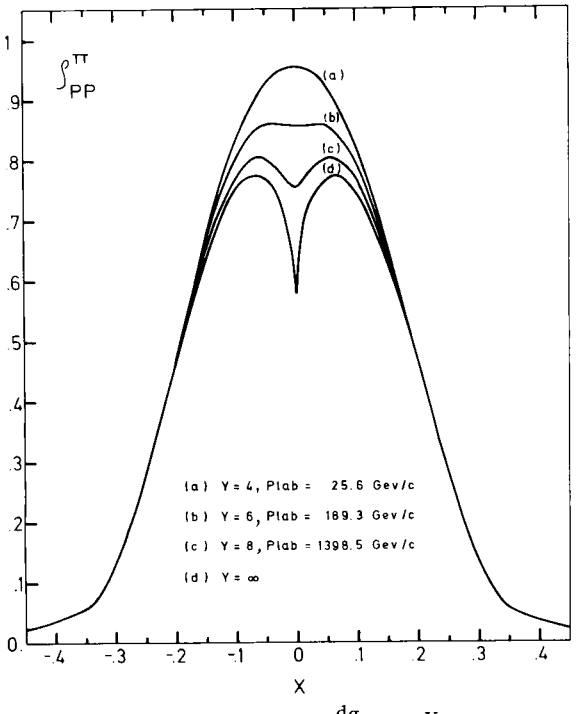

Fig. 5. Inclusive spectrum $\rho^{\pi}_{pp}(x) = \int x \frac{d\sigma_{pp \to \pi X}}{dx d^2p_\perp} d^2p_\perp$ as a function of x.

The spectra at $Y = 4, 6, 8$ and ∞ are shown in fig. 3 as a function y_{lab}, in fig. 4 as a function of $y_{c.m.}$ and in fig. 5 as a function of x. The x-spectrum is obtained from the y-spectrum * using $\langle p_\perp \rangle = 0.350$ GeV/c. In this approximation a different value of $\langle p_\perp \rangle$ is only a change on the scale of x. For instance, $\langle p_\perp \rangle \to 0.550$ GeV/c gives $x \to 1.5x$.

Thus, fig. 3, 4 and 5 shows the limits of fragmentation of a into π, pionization and scaling, respectively.

It can be observed that the fragmentation limit is approached much faster than the pionization one, or conversely, that the scaling limit is approached much faster for larger $|x|$, as it is stated in sect. 2.

The spectrum at $x = 0$ is observed to rise with the energy up to 30 GeV/c and then to go slowly down to the asymptotic value of 0.585. At 1500 GeV/c there is a 7% dip and at $s = \infty$ there is a 26% dip.

The average multiplicity of pions $\bar{n}_\pi$ and the average number of exchanged pomerons $\bar{n}_P$ are given by

* See footnote on page 225.

$$\bar{n}_\pi = \frac{1}{\sigma_{ab}^{tot}}\left(g_{PM}^2 \frac{\partial}{\partial g_{PM}^2} + g_{MM}^2 \frac{\partial}{\partial g_{MM}^2}\right)\sigma_{ab}^{tot},$$
$$\bar{n}_P = \frac{1}{2\sigma_{ab}^{tot}}\left(g_{PM}^2 \frac{\partial}{\partial g_{PM}^2} + G_{a,P}^2 \frac{\partial}{\partial G_{a,P}^2} + G_{b,P}^2 \frac{\partial}{\partial G_{b,P}^2}\right)\sigma_{ab}^{tot}. \quad (42)$$

At large values of Y they behave as

$$\bar{n}_\pi = (0.585 + 0.441\, e^{-\frac{1}{2}Y})\, Y + 0.665 - 9.070\, e^{-\frac{1}{2}Y},$$
$$\bar{n}_P = (0.074 - 0.380\, e^{-\frac{1}{2}Y})\, Y + 0.193 + 1.595\, e^{-\frac{1}{2}Y}. \quad (43)$$

These results should not be taken as an accurate prediction but rather as an illustration of what we expect to happen. The experimental $y_\pi < y_a$ and $y_\pi > y_b$ tails are not reproduced, but we expect these regions of phase space to be dominantly populated by diagrams with baryon exchange and/or transverse momenta smaller than the average one we used, as we discuss in sect. 6. In addition, the kernel given in eq. (17) would probably give a bigger contribution in those regions.

4. COMPARISON WITH OTHER MODELS

In this section we want to show that the $f = A + B\sqrt{x} + 0(x)$ structure in the scaling function is also present in macroscopic models and to study to which element of the MP model is that cusp related.

According to Mueller's analysis [3] the spectrum of c in the reaction a+b → c+X is proportional to the discontinuity in the missing mass squared M_x^2 of the forward a + b + $\bar{c}$ → a + b + $\bar{c}$ amplitude as depicted in fig. 6. Regge behavior for this amplitude at large $p_a \cdot p_c$ and $p_b \cdot p_c$ gives

$$\frac{d\sigma_{ab}}{dy_c d^2 p_c^\perp} = \lambda^{-\frac{1}{2}}(s, m_a^2, m_b^2) \sum_{rr'} \gamma_a^r \gamma_b^{r'} \Gamma_{rr'}^c(p_\perp^c)\,(p_a \cdot p_c)^{\alpha_r(0)} \times (p_b \cdot p_c)^{\alpha_{r'}(0)}. \quad (43)$$

Since

$$p_a \cdot p_c = m_a\, \omega_c \cosh(y_c - y_a) \cong \tfrac{1}{2}\, m_a\, \omega_c\, e^{y_c - y_a},$$
$$p_b \cdot p_c = m_b\, \omega_c \cosh(y_b - y_c) \cong \tfrac{1}{2}\, m_b\, \omega_c\, e^{y_b - y_c}, \quad (44)$$

eq. (43) is equivalent to eq. (32), and therefore at small x it is $f_i^c(x) = A + B\sqrt{x} + O(x)$, with B proportional to $\Sigma_R\, \gamma_i^R \Gamma_{RP}^c$

Let us now go back to the MP model. The model discussed in last section has two exchanges and gives

$$f_i^{\pi}(x) = f^{\pi} + \frac{\gamma_i^{\mathrm{R}}}{\gamma_i^{\mathbb{P}}} h^{\pi}(m_i x/\bar{\omega}_{\pi})^{\frac{1}{2}}, \tag{45}$$

where h^{π} is independent of particle i. Therefore in this model the amount of cusp is proportional to the amount of secondaries σ_{ab}^{tot}. This, however, is too rough an approximation since in Regge phenomenology the $s^{-\frac{1}{2}}$ coefficient in σ^{tot} is generally given by the sum of the residues of *several* poles, which can have different signs.

We want then to discuss a MP model with three exchanges so as to produce two output poles with intercept close to 0.5. We choose the three exchanges to be a meson (M) baryon (B) and antibaryon ($\bar{\mathrm{B}}$); vacuum exchange is allowed to contribute only to the elastic amplitude, as opposed to the model discussed in sect. 3.

This model was proposed by Ting [10] to account for the difference $\Delta\sigma = \sigma_{\bar{p}p}^{tot} - \sigma_{pp}^{tot}$. However, the same discussion can be applied to study $K\bar{K}$ production changing $N \to K$ and $B \to S$ (strangeness exchange) [11].

In the terminology of sect. 2 the model is given by

$$G_{\mathrm{N}}^2 = (G_{\mathrm{M}}^2\ G_{\mathrm{B}}^2\ 0) = (\tilde{G}_{\bar{\mathrm{N}}}^2)^{\mathrm{T}}, \quad G_{\bar{\mathrm{N}}}^2 = (G_{\mathrm{M}}^2\ 0\ G_{\mathrm{B}}^2) = (\tilde{G}_{\mathrm{N}}^2)^{\mathrm{T}}, g^2 = g_{\pi}^2 + g_{\mathrm{B}}^2,$$

$$g_{\pi}^2 = \begin{pmatrix} g_{\mathrm{MM}}^2 & 0 & 0 \\ 0 & g_{\mathrm{BB}}^2 & 0 \\ 0 & 0 & g_{\mathrm{BB}}^2 \end{pmatrix} \qquad g_{\mathrm{B}}^2 = \begin{pmatrix} 0 & g_{\mathrm{BM}}^2 & g_{\mathrm{BM}}^2 \\ g_{\mathrm{BM}}^2 & 0 & 0 \\ g_{\mathrm{BM}}^2 & 0 & 0 \end{pmatrix}, \tag{46}$$

$$K(Z) = \begin{pmatrix} K_{\mathrm{M}}(Z) & 0 & 0 \\ 0 & K_{\mathrm{B}}(Z) & 0 \\ 0 & 0 & K_{\mathrm{B}}(Z) \end{pmatrix}.$$

The vertex g_{π}^2 corresponds to pion production and the vertex g_{B}^2 to baryon or antibaryon emission in position other than the ends of the MP chain. At least three output poles are obtained which Ting identifies with $\mathbb{P}$, $\mathbb{P}'$ and ω *.

Then, at large values of s

$$\begin{aligned} \sigma_{p\bar{p}} &\sim \gamma_{\mathbb{P}}^2 + s^{-\frac{1}{2}}(\gamma_{\mathbb{P}'}^2 + \gamma_{\omega}^2), \\ \sigma_{pp} &\sim \gamma_{\mathbb{P}}^2 + s^{-\frac{1}{2}}(\gamma_{\mathbb{P}'}^2 - \gamma_{\omega}^2) \end{aligned} \tag{47}$$

The scaling functions, at small values of x, are given by

$$\begin{aligned} f_{\mathrm{p}}^{\pi}(x) &= f_{\mathrm{p}}^{\pi}(x) = f^{\pi} + \Gamma_{\mathbb{P}\mathbb{P}'}^{\pi}\sqrt{x} + \mathrm{O}(x), \\ f_{\mathrm{p}}^{\mathrm{p}}(x) &= f_{\bar{\mathrm{p}}}^{\bar{\mathrm{p}}}(x) = f^{\mathrm{B}} + (\Gamma_{\mathbb{P}\mathbb{P}'}^{\mathrm{B}} + \Gamma_{\mathbb{P}\omega}^{\mathrm{B}})\sqrt{x} + \mathrm{O}(x), \end{aligned} \tag{48}$$

* Exchange degeneracy between $\mathbb{P}'$ and ω is obtained only for $g_{\mathrm{BM}}^2 = 0$, but in the text we make $\mu_{\mathbb{P}'} \sim \mu_{\omega} \sim 0.5$ for simplicity since $\mu_{\mathbb{P}'} - \mu_{\omega} = \mathrm{O}(g_{\mathrm{BM}}^4)$.

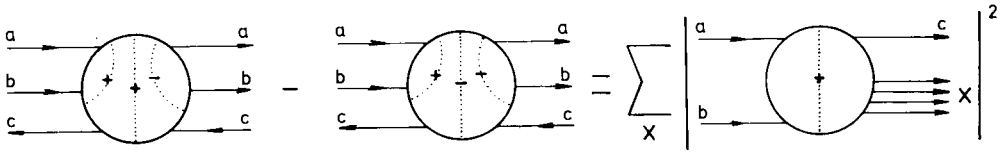

Fig. 6. The a + b → c + X cross section as the discontinuity of the a + b + c → a + b + c amplitude.

$$f_{\bar{p}}^{\bar{p}}(x) = f_{\bar{p}}^{p}(x) = f^{B} + (\Gamma^{B}_{\mathbb{P}\mathbb{P}'} - \Gamma^{B}_{\mathbb{P}\omega})\sqrt{x} + O(x),$$

where

$$\begin{aligned} f^{\pi} &= O(g^2_{MM}), \\ f^{B} &= O(g^4_{MB}), \\ \Gamma^{c}_{rr'} &= O(g^2_{MB}) \end{aligned} \tag{49}$$

We thus see that the amount of cusp in $f_i^c(x)$ is controlled by g^2_{BM} rather than by the amount of secondaries in σ_{ab}. Namely, if we make $g^2_{MB} = 0$, the cusps in the three scaling functions disappear and $\gamma^2_{\mathbb{P}'} \to \gamma^2_{\omega}$, making the coefficient of $s^{-\frac{1}{2}}$ in σ_{pp} –but not in $\sigma_{\bar{p}p}$ – vanish.

It is easy to see why there can be secondaries in $\sigma_{\bar{p}\bar{p}}$ and no cusp in the scaling functions: the difference $\Delta\sigma$ is given by the set of diagrams with only baryon exchange. These diagrams cannot produce a cusp in $f_i^c(x)$ and are independent of g^2_{BM}.

This way we learn that in the MP model the cusp is related to the interference between different (input) poles, i.e., to the non-diagonal elements of g^2.

Before leaving this model we observe that it leads to two non-obvious predictions for the $\bar{p}p$ annihilation process, that cannot be extracted from macroscopic models:

(i) $\Delta\sigma = \sigma_{\bar{p}p} - \sigma_{pp} = \sigma^{ann.}_{\bar{p}p}$.

(ii) Scaling behavior for a "partially inclusive" process, namely the spectrum of pions coming from $p\bar{p}$ annihilation defined as

$$\rho^{\pi,\,ann}_{\bar{p}p}(x, p_\perp, s) = \frac{E^{\pi}}{\sigma^{ann}_{\bar{p}p}} \frac{d\sigma^{ann}_{\bar{p}p}}{d^3 p_\pi} \tag{50}$$

scales for $s \to \infty$.

Notice that this statement is not true if in eq. (50) we divide by $\sigma^{tot}_{\bar{p}p}$ instead of by $\sigma^{ann}_{\bar{p}p}$.

Let us make this point more clear with another example: consider the spectrum of the lambda or of the pions coming from the process K + p → Λ + (pions). It is predicted to scale if we divide by

$$\sigma(K + p \to \Lambda + (\text{pions})) = \sum_n \sigma(K + p \to \Lambda + n\pi) \tag{51}$$

and not to scale if we divide by σ^{tot}_{Kp}, since in the MP model the cross section (51) is expected to vanish as some negative power of s. This is the same prescription we gave in sect. 1 for the strictly inclusive cross section to account for the possibility

of vanishing or divergent asymptotic total cross section.

As a consequence of scaling for the spectrum (50) the average multiplicity of pions coming from $\bar{p}p$ annihilation events grows linearly with $\log s$.

5. TWO PARTICLE INCLUSIVE SPECTRUM

For the inclusive process $a + b \to c + d + X$ we define

$$\rho_{a,b}^{c,d}(\boldsymbol{p}_c, \boldsymbol{p}_d, s) = \frac{E^c E^d}{\sigma_{ab}^{tot}} \frac{d\sigma_{ab}}{d^3\boldsymbol{p}_c d^3\boldsymbol{p}_d} . \tag{52}$$

In order to study its limiting properties, as predicted by the MP model, as $S \to \infty$, we distinguish eleven different regions in the (y_c, y_d) plane at fixed $p_\perp^c$, $p_\perp^d$ and φ, where $\boldsymbol{p}_\perp^c \cdot \boldsymbol{p}_\perp^d = p_\perp^c p_\perp^d \cos\varphi$. (See fig. 7) The asymptotic dependence on the different particles is shown in table 1.

In the same table it is shown that $\rho_{a,b}^{c,d}$ scales, namely

$$\lim_{s \to \infty} \rho_{a,b}^{c,d}(\boldsymbol{p}_c, \boldsymbol{p}_d, s) = f_{a,b}^{c,d}(x_c, x_d, p_c^\perp, p_d^\perp, \varphi) \tag{53}$$

if we exclude the point $(x_c, x_d) = (0,0)$ *. The reason for this is very simple: regions 9, 10 and 11 are concentrated in this point; the first of which depends on the short range correlation between c and d. Therefore $f_{a,b}^{c,d}$ tends to different values when $(x_c, x_d) \to (0,0)$ along different paths in the (x_c, x_d) plane.

Table 1

Limiting properties of the $a + b \to c + d + X$ spectrum as predicted by the MP model.

	FIXED VARIABLES	$\lim_{S\to\infty} \varrho_{a,b}^{c,d}(\vec{p}_c, \vec{p}_d, S)$	x_c	x_d	$f_{a,b}^{c,d}(x_a, x_d, p_c^\perp, p_d^\perp, \varphi)$
1	$y_c - y_a$, $y_b - y_d$	$\varrho_a^c(y_c - y_a, p_c^\perp)\varrho_b^d(y_b - y_d, p_d^\perp)$	−	+	$f_a^c(-x_c, p_c^\perp) f_b^d(x_d, p_d^\perp)$
2	$y_d - y_a$, $y_b - y_c$	$\varrho_a^d(y_d - y_a, p_d^\perp)\varrho_b^c(y_b - y_c, p_c^\perp)$	+	−	$f_a^d(-x_d, p_d^\perp) f_b^c(x_c, p_c^\perp)$
3	$y_b - y_c$, $y_b - y_d$	$\varrho_b^{c,d}(y_b - y_c, y_b - y_d, p_c^\perp, p_d^\perp, \varphi)$	+	+	$f_b^{c,d}(x_c, x_d, p_c^\perp, p_d^\perp, \varphi)$
4	$y_c - y_a$, $y_d - y_a$	$\varrho_a^{c,d}(y_c - y_a, y_d - y_a, p_c^\perp, p_d^\perp, \varphi)$	−	−	$f_a^{c,d}(-x_c, -x_d, p_c^\perp, p_d^\perp, \varphi)$
5	$y_c^{c.m.}$, $y_b - y_d$	$\varrho^c(p_c^\perp)\varrho_b^d(y_b - y_d, p_d^\perp)$	0	+	$f^c(p_c^\perp) f_b^d(x_d, p_d^\perp)$
6	$y_c^{c.m.}$, $y_d - y_a$	$\varrho^c(p_c^\perp)\varrho_a^d(y_d - y_a, p_d^\perp)$	0	−	$f^c(p_c^\perp) f_a^d(-x_d, p_d^\perp)$
7	$y_d^{c.m.}$, $y_b - y_c$	$\varrho^d(p_d^\perp)\varrho_b^c(y_b - y_c, p_c^\perp)$	+	0	$f^d(p_d^\perp) f_b^c(x_c, p_c^\perp)$
8	$y_d^{c.m.}$, $y_c - y_a$	$\varrho^d(p_d^\perp)\varrho_a^c(y_c - y_a, p_a^\perp)$	−	0	$f^d(p_d^\perp) f_a^c(-x_c, p_c^\perp)$
9	$y_c - y_d$; $y_a \ll y_c \ll y_d$	$\varrho^{c,d}(\lvert y_d - y_c\rvert, p_c^\perp, p_d^\perp, \varphi)$	0	0	
10	$y_a \ll y_c \ll y_d \ll y_b$	$\varrho^c(p_c^\perp)\varrho^d(p_d^\perp)$	0	0	
11	$y_a \ll y_d \ll y_c \ll y_b$		0	0	

* As a function of the variables $x_{cd} = (x_c^2 + x_d^2)^{\frac{1}{2}}$ and $\theta_{cd} = \tan^{-1}(x_c/x_d)$, ρ_{ab}^{cd} scales even at $x_{cd} = 0$.

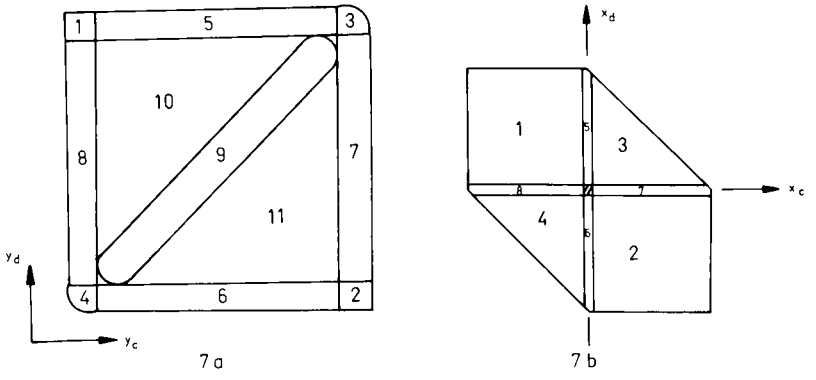

Fig. 7. Phase space for the inclusive process a+b → c+d+X at a large value of Y. The numbers denote regions with different limiting properties according to table 1. (a) In the rapidities (y_c,y_d) plane. The width of regions 5 to 9 is the correlation length. (b) In The (x_c,x_d) plane. When $Y \to \infty$ regions 9 to 11 become the point $x_c = x_d = 0$.

The integral

$$\int \rho_{a,b}^{c,d}\, dy_c dy_d d^2\boldsymbol{p}_c^{\perp}\, d^2\boldsymbol{p}_d^{\perp} \tag{54}$$

equals $\langle n_c n_d \rangle$ if particles c and d are of different type, or $\langle n_c(n_c-1)\rangle$ if they are of the same type.

Since the main contribution to that integral comes from regions 10 and 11, the mean square deviation of multiplicity n_c grows linearly with log s, i.e.

$$\langle (n_c - \langle n_c \rangle)^2 \rangle = O(\ln s). \tag{55}$$

In the model described in sect. 2 the spectrum for a + b → π + π + X is given by

$$\rho_{a,b}^{\pi,\pi} = \frac{1}{\sigma_{ab}} G_a^2 A(y_{\pi_1} - y_a - \bar{\Delta}_a) g^2 A(y_{\pi_2} - y_{\pi_1}) g^2 A(y_b - y_{\pi_2} - \bar{\Delta}_b) \tilde{G}_b^2 + (1 \leftrightarrow 2), \tag{56}$$

when none of the pions is emitted at the end positions on the MP chain. This function has the limiting properties described in table 1.

6. IMPROVEMENTS TO THE MODEL

Two major approximations were done in sect.2

(a) Ignoring transverse momenta.

(b) Neglecting the contribution of the particles emitted at both ends of the MP chain to the inclusive spectrum.

These approximations lead to expressions where the total and inclusive cross sec-

tions are directly given by the solution of the integral eq. (24) with no further integrations, making it possible to perform a fit with a computer in a reasonable time.

Approximation (b) does not affect in general the central part of the spectrum and should be very good for the whole $p + p \to \pi^- + X$ spectrum, fitted in sect.3 *.

In this section we improve the model introducing the dependence on transverse momenta and the repidities of the end particles.

Eq. (16) shows that an amplitude that factorizes as a function of the invariant momentum transfer t_i yields a factorized dependence on the exchanged transverse momenta $\boldsymbol{q}_i = \Sigma_{j=0}^{i-1} \boldsymbol{p}_j^{\perp}$, though not on the $\boldsymbol{p}_i^{\perp}$. We thus complete the kernel in eq. (17) as

$$K_{i-1\,i} = \mathrm{e}^{-b(\omega_{i-1}\,\omega_i\,\mathrm{e}^{-Z+q_i^2})}\mathrm{e}^{-\beta Z}\alpha\, f(q_i) K_{\pi\pi}(Z-\eta_i-\eta_{i-1}+2\bar{\eta}_\pi) \tag{57}$$

where ω_i is not fixed at an average value but depends on $\boldsymbol{p}_i^{\perp} = \boldsymbol{q}_{i+1} - \boldsymbol{q}_i$.

The n-particle production cross section is given by

$$\begin{aligned} \mathrm{d}\sigma_{\mathrm{ab}}^n(Y) = {} & G_{\mathrm{a}}^2(\epsilon_{\mathrm{a}}, q_1)\, f(q_1) K(Z_{\mathrm{i}}) g^2 \ldots K(Z_{n+1})\, \tilde{G}_{\mathrm{b}}^2(\epsilon_{\mathrm{b}}, q_{n+1}) \\ & \times\ \delta(Y-\Delta-\sum_{i=1}^{n+1} Z_i) \prod_{i=1}^{n+1} (\mathrm{d}Z_i\, \mathrm{d}^2 q_i), \end{aligned} \tag{58}$$

where

$$\begin{aligned} & f(q) = b\, \mathrm{e}^{-bq^2}/\pi, \qquad \eta_i = \bar{\eta}_i + \ln \frac{\omega_i}{\bar{\omega}_i}, \\ & \Delta = \epsilon_{\mathrm{a}} + \epsilon_{\mathrm{b}} + \eta_0 + 2\sum_{i=1}^{n} \eta_i + \eta_{n+1} - 2(n+1)\,\bar{\eta}_\pi, \end{aligned} \tag{59}$$

with ϵ_i given eq. (11).

All the expressions of sect.2, with $G_i^2 = \int G_i^2(\bar{\epsilon}_i, q)\, f(q)\, \mathrm{d}^2 q$, can be obtained integrating over all $\mathrm{d}^2 \boldsymbol{q}_i$ and setting $\epsilon_i \sim \bar{\epsilon}_i$, $\eta_i \sim \bar{\eta}_i$. In this section we follow the same recipe except for the observed momentum $p_j^{\perp}$, for which we use the actual value η_j.

The cross section for $a + b \to \pi + X$ when the pion is not emitted at end position of the MP chain is thus given by

$$\frac{\mathrm{d}\sigma_{\mathrm{ab}}}{\mathrm{d}y \mathrm{d}^2 p_\perp} = G_{\mathrm{a}}^2 A\left(y - y_{\mathrm{a}} - \bar{\Delta}_{\mathrm{a}} - \ln\frac{\omega_\pi}{\bar{\omega}_\pi}\right) g^2 A\left(y_{\mathrm{b}} - y - \bar{\Delta}_{\mathrm{b}} - \ln\frac{\omega_\pi}{\bar{\omega}_\pi}\right) \tilde{G}_{\mathrm{b}}^2\, F^\pi(p_\perp^2), \tag{60}$$

where ω_π is the longitudinal mass of the observed pion and

$$F^\pi(p_\perp^2) = \int \mathrm{d}^2 q_1\, \mathrm{d}^2 q_2\, \delta^{(2)}(\boldsymbol{p}_\perp - \boldsymbol{q}_1 + \boldsymbol{q}_2)\, f(q_1)\, f(q_2) = b\, \mathrm{e}^{-\frac{1}{2}bp_\perp^2}/2\pi, \tag{61}$$

which gives $b \sim 2/\langle p_\perp^2 \rangle$.

The inclusive spectrum as a function of x and $p_\perp$ and the scaling function are obtained from (60) with no further approximations. An interesting result is that the

* If one is interested in the $p+p \to \pi^+ + X$ spectrum baryon exchange cannot be neglected and thus there is some contribution from π^+ emitted at end positions of the MP chain. See ref. [14].

scaling function factorizes as

$$f_i^{\pi}(x, p_\perp) = f_i^{\pi}(x)\, F^{\pi}(p_\perp^2), \tag{62}$$

with $f_i^{\pi}(x)$ given eq. (34).

Another prediction of eq. (60) is that the scaling limit, at fixed $p_\perp^2$, is approached faster for smaller values of $p_\perp^2$.

We finally consider the spectrum of a particle emitted at an end position in the MP chain, as depicted in fig. 8a. In sect.2 we integrated over dy_0 and dy_{n+1} making use of the δ functions of conservation of energy and longitudinal momentum, and argued that, in the MP region, $y_0(y_{n+1})$ depends mainly on $y_a(y_b)$, being quite independent of the momenta of the other particles.

Similarly, here we integrate over dy_1 and dy_{n+1} and argue that, in the MP region, y_{n+1} depends mainly on y_b and y_1 on y_a and y_0 through the relation

$$\bar{\omega}_1\, e^{-\bar{y}_1} \cong m_a\, e^{-y_a} - \omega_0\, e^{-y_0} \tag{63}$$

We then integrate over the momenta of the other particles and sum over n, obtaining

$$\frac{d\sigma_{ab}}{dy_0 d^2\boldsymbol{p}_0^\perp} = \frac{\omega_0}{\bar{\omega}_1} e^{\bar{y}_1 - y_0} G_a^2(y_0 - y_a, p_0^\perp) f(p_0^\perp) K(y_1 - y_0 - \eta_0) g^2 A(y_b - y_1 - \bar{\Delta}_b) \tilde{G}_b^2. \tag{64}$$

Another pair of variables commonly used are $t = (p_a - p_0)^2$ and $M^2 = (p_a + p_b - p_0)^2$. The triple Regge (TR) limit is defined as t fixed, $M^2 \to \infty$, $s/M^2 \to \infty$ and gives

$$y_b - \bar{y}_1 \sim \ln \frac{M^2}{\omega_1 m_b}, \quad \bar{y}_1 - y_a \sim \ln \frac{s\bar{\omega}_1}{M^2 m_a}, \quad t \sim -(p_0^\perp)^2. \tag{65}$$

In this limit expression (64) tends to

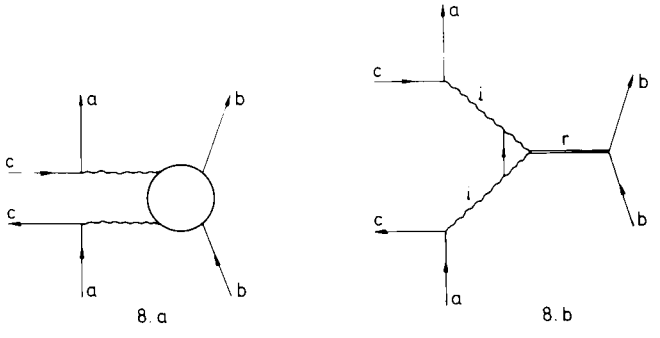

Fig. 8. (a) The cross section a+b → c+X when particle c is emitted at the first position in the MP chain. (b) The same diagram in the triple Regge limit, in the MP model.

$$\frac{d\sigma_{ab}}{dtdM^2} = \frac{\pi}{s}\frac{d\sigma_{ab}}{dy_0 d^2p_0^{\perp}} \cong \frac{1}{16\pi s^2}\sum_{i,r} |\beta_{a,i}(t)|^2 \left(\frac{s}{M^2}\right)^{2\alpha_i(t)} g_{r,ii}(t)\left(\frac{M^2}{s_0}\right)^{\alpha_r(0)} \tilde{\beta}^r_b, \tag{66}$$

where the residues are normalized by

$$\frac{d\sigma^{el}_{ab}}{dt} \cong \frac{1}{16\pi s^2}\sum_i |\beta_{a,i}(t)|^2 \left(\frac{s}{s_0}\right)^{2\alpha_i(t)} |\beta_{b,i}(t)|^2,$$
$$\sigma^{tot}_{ab} \cong \frac{1}{s}\sum_r \tilde{\beta}^r_a \left(\frac{s}{s_0}\right)^{\alpha_r(0)} \tilde{\beta}^r_b. \tag{67}$$

The TR coupling parameter defined by

$$\eta_{r,ii}(t) = \frac{S_0}{16\pi}\frac{g^2_{r,ii}(t)}{2\alpha'_P} \tag{68}$$

is given in the model by

$$\eta_{r,ii}(t) = \Omega_{r,ii}\frac{e^{2t/\langle p_\perp^2\rangle}}{\langle p_\perp^2\rangle 2\alpha'_P}\left(\frac{s_0}{\omega_\pi^2}\right)^{\alpha_r(0)+1-2\alpha_i(t)}, \tag{69}$$

with $\Omega_{r,ii} = 2\left(\sum_j C_{r,j}\, g^2_{ji}\right)^2$.

In the fit of sect.3 we made use of two input poles (P and M) and two output poles (**P** and R). Therefore there are four TR vertices, namely

$$\Omega_{\mathbf{P},PP}=0.026, \quad \Omega_{R,PP}=0.20, \quad \Omega_{\mathbf{P},MM}=4.38,$$
$$\Omega_{R,MM}=14.0. \tag{70}$$

Both $\eta_{\mathbf{P},PP}$ and $\eta_{R,PP}$ turned out to be small in accordance with theoretical predictions [12]. The fact that the firgures in eq.(70), when used in eq.(69), are consistent with evaluations of η_{PPP} in the TR limit [13] is encouraging since they were obtained from a fit of the $p+p \to \pi+X$ spectrum in which there is no contributions from any of those vertices, in the TR limit.

7. CONCLUSIONS

The MP model was shown to be consistent with the shape of the longitudinal inclusive pion spectrum in pp collision at around 30 GeV. The extrapolation of the

model with the inclusion of Meson and Pomeron exchanges to ISR energies shows the appearance of a dip in the x variable which asymptotically develops into an inverted cusp of the form $A + B\sqrt{|x|}$. In the rapidity variable a central plateau is shown to develop quite slowly. These features are discovered in other versions of the MP model and the importance of the cusp is shown to depend on the coupling between different input channels. They are also consistent with Mueller's analysis with the inclusion of Regge secondaries.

It was also shown that the MP model predicts scaling behavior for certain partially inclusive processes when the spectra are properly normalized.

The predictions of the MP model for the limiting properties of the two-particle inclusive spectrum were also discussed. In particular it was shown that the spectrum has scaling behavior if one excludes the point $x_1 = x_2 = 0$.

The author wants to express his gratitude to Alberto Pignotti for his help and guidance, and to the colleagues of the Laboratorio del Sincrociclotrón, Comisión Nacional de Energía Atómica, for encouragement and help.

REFERENCES

[1] R.P. Feynman, Phys. Rev. Letters 23 (1969) 1415.
[2] J. Benecke, T.T. Chou, C.N. Yang and E. Yen, Phys. Rev. 188 (1969) 2159.
[3] A.H. Mueller, Phys. Rev. D2 (1970) 2963.
[4] C. de Tar, Phys. Rev. D3 (1971) 138.
[5] D. Amati, S. Fubini and A. Stanghellini, Nuovo Cimento 26 (1962) 896.
[6] A Pignotti, Proc. of the Colloqium on multiparticle dynamics, Helsinki, May 1971, to be published;
see also F. Zachariasen and Zweig, Phys. Rev. 160 (1967) 1322.
[7] A. Pignotti and P. Ripa, Phys. Rev. Letters 27 (1971) 1538.
[8] A.C. Aitken, Determinants and matrices (Oliver and Boyd, London 1956) p. 48.
[9] G.F. Chew and D.R. Snider, Phys. Rev. D1 (1970) 3453.
[10] P.D. Ting, Phys. Rev. 181 (1969) 1942.
[11] I. Gyuk and D.R. Snider, University of Wisconsin, Maryland, preprint UWM–4867–71–5; D. Snider, UWM–4867–71–10.
[12] H.D.I. Abarbanel, G.F. Chew, M.L. Goldberger and L.M. Saunders, Phys. Rev. 26 (1971) 937 for η_{PPP};
M.B. Einhorn, B.B. Green and M.A. Virasoro, Phys. Letters 37B (1971) 292 for η_{RPP}.
[13] R. RAjamaran, Phys. Rev. Letters, 27 (1971) 693;
see also S. Miyake and A. Takahashi, Tohoku University preprint (Sept. 1971).
[14] L. Caneschi and A. Pignotti, Phys. Rev. 22 (1969) 1219.